

3. Aerosol, Radiation, Ozone, and Water Vapor Division

B. BODHAINE, E. DUTTON, R. EVANS, R. GRASS, J. HARRIS, D. HOFMANN, W. KOMHYR,
D. NELSON, J. OGREN, AND S. OLTMANS

3.1. CONTINUING PROGRAMS

3.1.1. SURFACE AEROSOLS

3.1.1.1. BASELINE OBSERVATIONS

Operations

The aerosol monitoring program at BRW, MLO, and SPO continued during 1993 as in previous years. CN concentration was measured continuously with TSI (butanol-based) CN counters at BRW, MLO, and SPO. Daily calibration points were provided by Pollak CN counters at all stations. Aerosol scattering extinction coefficient (σ_{sp}) at 450-, 550-, 700-, and 850-nm wavelengths was measured continuously at BRW, MLO, and SPO with four-wavelength nephelometers. Aerosol absorption coefficient has been measured continuously using aethalometers at BRW since April 1988, MLO since April 1990, and at SPO during December 1986-December 1991.

Figure 3.1 shows daily geometric means of CN concentration (lower portion of each plot), σ_{sp} (middle portion of each plot), and Ångström exponent (upper portion of each plot) at the BRW, MLO, and SPO stations for 1993. Two independent values of Ångström exponent (α) were calculated from the 450-, 550-, and 700-nm channels of σ_{sp} data using the relation $\alpha = -\Delta \log \sigma_{sp} / \Delta \log \lambda$, where α is Ångström exponent and λ is wavelength. These averages were calculated only if data for all three wavelengths were available. A graphical presentation of the monthly geometric means of the entire data record for BRW, MLO, and SPO is shown in Figure 3.2. Monthly geometric means of the 1993 aerosol data are listed in Table 3.1.

Discussion

The BRW data in Figure 3.1 show a σ_{sp} maximum of about $3 \times 10^{-5} \text{ m}^{-1}$ during spring, typical of the well-known Arctic haze. Minimum values of σ_{sp} below 10^{-6} m^{-1} occurred in July-August. The BRW long-term record shown in Figure 3.2 clearly shows this annual cycle in σ_{sp} , with springtime monthly means of about 10^{-5} m^{-1} and summertime monthly means of about 10^{-6} m^{-1} . The BRW CN record shows a more variable semiannual cycle with a maximum that usually coincides with the maximum in σ_{sp} and a secondary maximum in late summer or early fall. The 1993 annual geometric mean for CN is 195 cm^{-3} (compared with 228 cm^{-3} for 1992) and the annual mean for σ_{sp} (550 nm) is $4.85 \times 10^{-6} \text{ m}^{-1}$ (compared with $4.62 \times 10^{-6} \text{ m}^{-1}$) for 1992. Note that the G.E. counter CN record is shown as a solid line and the TSI counter CN record is shown as a dashed line. The individual squares plotted on the CN graph are monthly means of Pollak

counter observations. These are shown separately because the TSI and Pollak counter give independent data sets, whereas the G.E. counter was calibrated using the Pollak counter data. Gaps in the data are apparent because of the averaging process that excludes data if local pollution is evident or if wind direction is not from the clean air sector. The BRW aerosol data set was presented by Bodhaine [1989] and Quakenbush and Bodhaine [1986].

The MLO σ_{sp} data shown in Figure 3.1 are typical of the long-term record, with the highest values in April and May, and lower values in fall and winter. Large events are apparent in the springtime, caused by the long-range transport of Asian desert dust in the upper troposphere to the vicinity of Hawaii. As discussed in the 1988 Summary Report [Elkins and Rosson, 1989], σ_{sp} values were generally higher since the installation of the new nephelometer in 1985 and have not reached the low values expected in winter. The MLO CN record shown in Figure 3.1 is typical, giving an annual geometric mean concentration of 381 cm^{-3} (compared with 375 cm^{-3} during 1992); the annual mean of σ_{sp} (550 nm) is $9.20 \times 10^{-7} \text{ m}^{-1}$ (compared with $8.58 \times 10^{-7} \text{ m}^{-1}$ during 1992). Note that all MLO aerosol data presented here are in the form of geometric means during 0000-0800 HST (1000-1800 UT) in order to include data for nighttime downslope wind conditions only. The MLO data set was presented by Massey *et al.* [1987]. A special study concerning aerosol measurements during the MLOPEX experiment is presented in section 3.2.2.

The SMO 1993 CN data are not presented because of problems associated with the sampling stack during that year. The SMO nephelometer was removed from service in March 1991. Future plans for the SMO aerosol program include a new humidity-controlled, size-controlled sampling system and a new multi-wavelength nephelometer.

The SPO σ_{sp} and CN data are shown in Figure 3.1. These data show a strong annual cycle reaching a maximum in the austral summer and a minimum in the austral winter, similar to previous years. The σ_{sp} data show events due to the transport of seasalt particles in winter but fairly clean values in the fall. Referring to the long-term data set for SPO shown in Figure 3.2, the σ_{sp} data generally show intermediate values in the austral summer and fall, and large events, sometimes exceeding 10^{-6} m^{-1} , in late winter. These large aerosol events are caused by the transport of seasalt in the upper troposphere from stormy regions near the Antarctic coast to the interior of the continent. The SPO 1993 annual means were about 90 cm^{-3} (69 cm^{-3} for 1992) for CN and $2.00 \times 10^{-7} \text{ m}^{-1}$ ($4.41 \times 10^{-7} \text{ m}^{-1}$ for 1992) for σ_{sp} (550 nm). The complete SPO data set was presented by Bodhaine and Shanahan [1990].

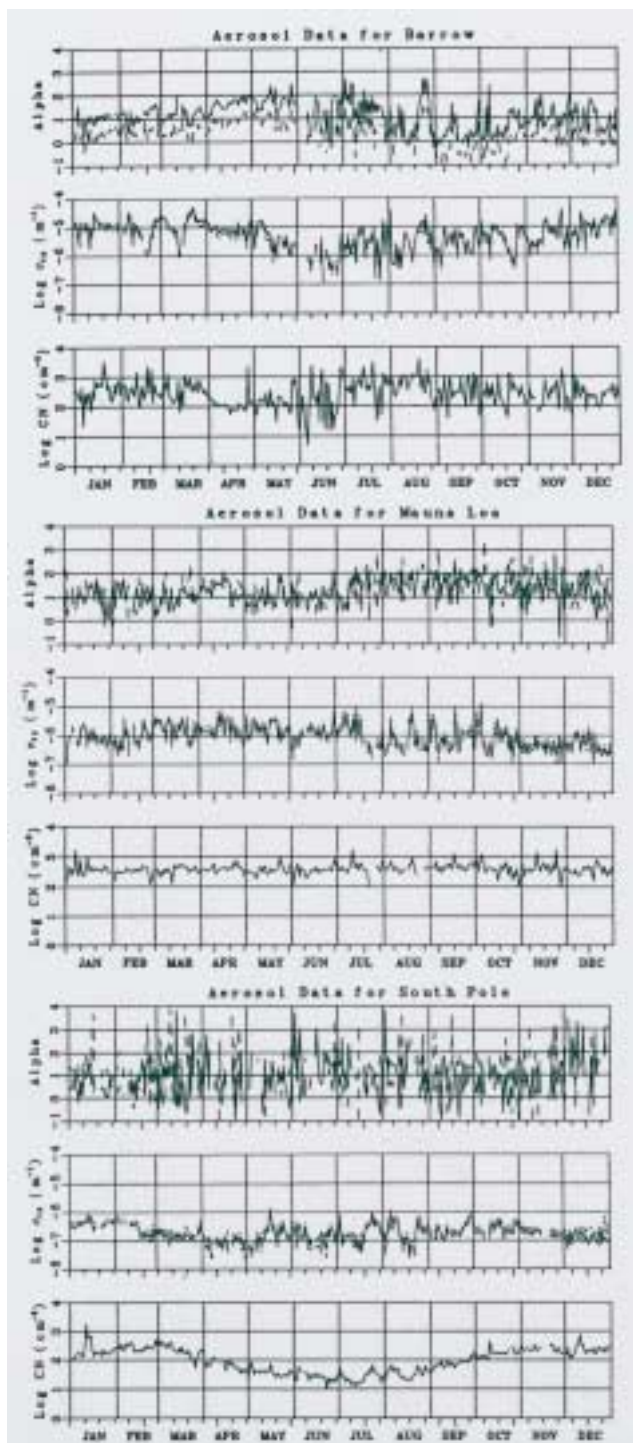


Fig. 3.1. Daily geometric means of σ_{sp} and CN data at BRW, MLO, and SPO for 1993. Data for MLO are included only for 0000-0800 HST. For each station, CN concentration (lower) is shown as a solid line and daily mean Pollak counter data are shown as small squares. σ_{sp} data (middle) are shown for 450 (dotted), 550 (solid), and 700 nm (dashed). Ångström exponents (alpha) were calculated from 450 and 550 nm (dotted) and 550 and 700 nm (solid) σ_{sp} data.

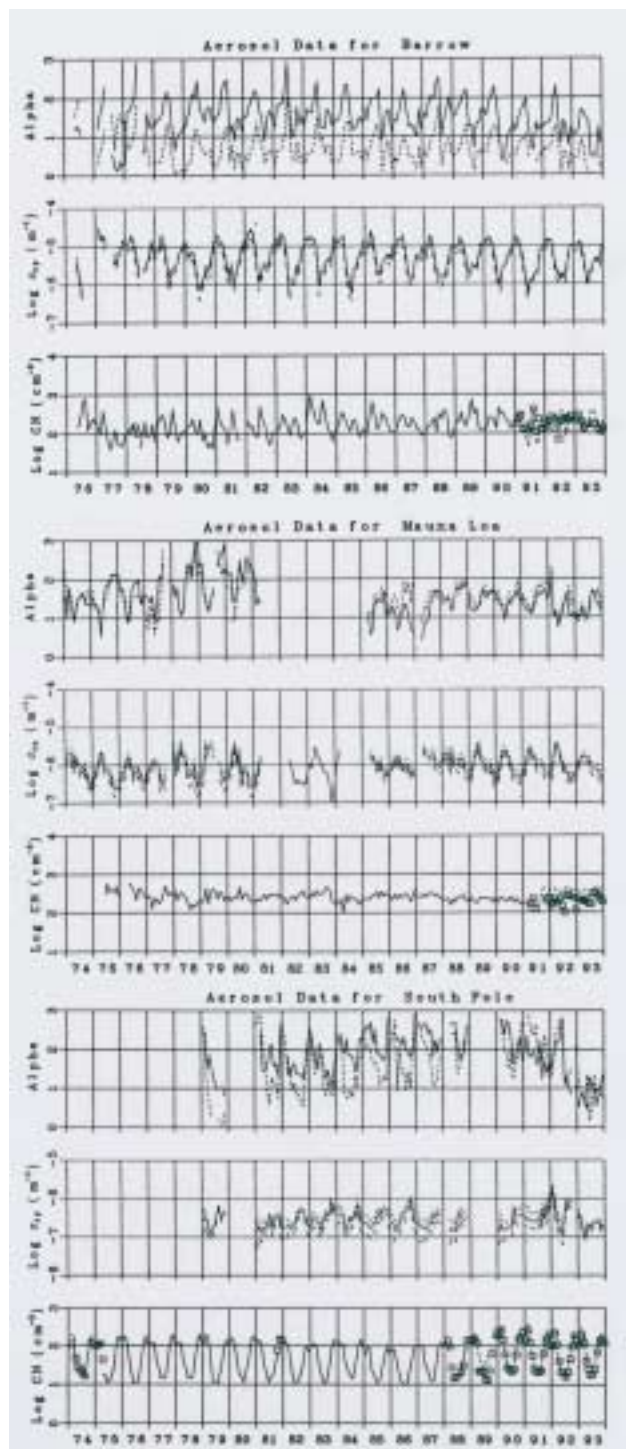


Fig. 3.2. Monthly geometric means of σ_{sp} and CN data for the entire data record at BRW, MLO, and SPO. Data for MLO are included only for 0000-0800 HST. σ_{sp} data (middle) are shown for 450 (dotted), 550 (solid), and 700 nm (dashed). Ångström exponents (alpha) were calculated from 450 and 550 nm (dotted) and 550 and 700 nm (solid) σ_{sp} data. Note that G.E. CN counter data are shown as a solid line, TSI CN counter data are shown as a dashed line, and Pollak CN counter data are shown as small squares.

TABLE 3.1. Monthly Geometric Means of CN concentration (cm^{-3}) and σ_{sp} (m^{-1}) at 450, 550, and 700 nm for BRW, MLO, and SPO During 1993

	Jan.	Feb.	March	April	May	June	July	Aug.	Sept.	Oct.	Nov.	Dec.
<i>BRW</i>												
CN	195	256	239	106	127	122	336	583	209	157	116	210
σ_{sp} (450)	1.22-5	9.62-6	1.59-5	9.86-6	5.03-6	7.09-7	2.33-6	2.51-6	3.28-6	5.70-6	3.57-6	1.10-5
σ_{sp} (550)	1.13-5	8.85-6	1.45-5	8.38-6	4.24-6	7.71-7	2.16-6	2.59-6	3.51-6	5.97-6	3.37-6	1.07-5
σ_{sp} (700)	8.74-6	6.81-6	1.10-5	5.73-6	2.82-6	5.90-7	1.44-6	2.25-6	3.16-6	5.39-6	2.55-6	8.79-6
<i>MLO</i>												
CN	385	321	364	407	353	347	396	403	473	367	411	363
σ_{sp} (450)	1.08-6	9.88-7	2.21-6	2.26-6	2.11-6	1.38-6	1.62-6	8.20-7	1.16-6	1.09-6	5.35-7	5.75-7
σ_{sp} (550)	8.71-7	8.17-7	1.79-6	1.69-6	1.74-6	1.14-6	1.28-6	5.86-7	8.39-7	7.99-7	3.76-7	4.55-7
σ_{sp} (700)	6.97-7	6.21-7	1.43-6	1.22-6	1.39-6	8.84-7	9.58-7	4.03-7	5.59-7	5.51-7	2.84-7	3.38-7
<i>SPO</i>												
CN	162	281	216	68	37	26	26	33	73	158	233	197
σ_{sp} (450)	5.01-7	3.26-7	2.03-7	1.06-7	2.03-7	1.85-7	2.31-7	2.88-7	2.67-7	3.03-7	2.32-7	1.87-7
σ_{sp} (550)	3.91-7	2.77-7	1.64-7	9.70-8	1.55-7	1.73-7	2.14-7	2.30-7	2.22-7	2.47-7	1.95-7	1.63-7
σ_{sp} (700)	3.46-7	2.27-7	1.36-7	7.95-8	1.48-7	1.28-7	1.62-7	1.74-7	1.95-7	2.09-7	1.60-7	1.11-7

A compact exponential format is used for σ_{sp} such that $1.22-5 = 1.22 \times 10^{-5}$.

3.1.1.2. REGIONAL OBSERVATIONS

In order to address questions concerning climate forcing by anthropogenic aerosol particles [Charlson *et al.*, 1992; Penner *et al.*, 1994], CMDL is establishing a network of regional aerosol monitoring stations. Two of the stations are located in marine locations and three in continental locations; for each category, one site is relatively free of anthropogenic influences and the others are frequently perturbed by anthropogenic aerosols. Table 3.2 lists the sites, their characteristics, and their status as of December 1993. Each station operates in close collaboration with a local university or government agency that provides onsite support for the measurements.

The scientific questions that define the context of the measurements at these sites include:

- What are the sign, mechanism, magnitude, uncertainty, and spatial distribution of the climate forcing by anthropogenic aerosol particles?
- What are the physical and chemical processes, including their rates and spatial distributions, leading to formation and removal of the particles responsible for the forcing, and how do these processes determine the size- and chemical-composition distributions of the particles?
- What is the sensitivity of the forcing and its spatial distribution to changes in these parameters?
- How has the forcing changed in the past, and how will it change in the future?

Clearly, ground based measurements at a few sites will provide answers to only a few of these questions.

Recognizing this, the strategy of the CMDL regional aerosol measurement program is *to determine means, variability, and possible trends of key optical, chemical, and microphysical properties for a number of important aerosol types*. The measurements will provide ground-truth for satellite measurements and global models, as well as key aerosol parameters for global-scale models (e.g., scattering efficiency of sulfate particles, hemispheric backscattering fraction). An important aspect of this strategy is that the chemical measurements are linked to the physical measurements through simultaneous, size-selective sampling and thermal analysis, which allows the observed aerosol properties to be connected to the atmospheric cycles of specific chemical species.

When the sites are fully operational, continuous measurements will include the total particle number concentration (N_{tot}), cloud condensation nucleus number concentration (N_{ccn}), aerosol optical depth (δ), and components of the aerosol extinction coefficient at one or more wavelengths (total scattering σ_{sp} , backwards hemispheric scattering σ_{bsp} , and absorption σ_{ap}). Size-resolved impactor and filter samples (submicrometer and supermicrometer size fractions) will be obtained for gravimetric and chemical (ion chromatographic, organic/elemental carbon) analyses. All size-selective sampling, as well as the measurements of the components of the aerosol extinction coefficient, will be performed at a low, controlled relative humidity (40%) to eliminate confounding effects because of changes in ambient relative humidity.

TABLE 3.2. Regional Aerosol Monitoring Sites

Category	Perturbed Marine	Perturbed Continental	Perturbed Continental	Clean Continental	Clean Marine
Location	Sable Is., Nova Scotia, Canada	Bondville, Illinois	K'puszta, Keszczemet, Hungary	Niwot Ridge, Colorado	Cheeka Peak, Washington
Designator	WSA	BND	KPO	NWR	CPO
Latitude	+43.933	+40.053	+46.967	+40.036	+48.30
Longitude	+060.007	+088.372	-019.550	+105.534	+124.62
Elevation (m)	5	230	180	3020	480
Collaborating Institute	Atmospheric Environment Service, Canada	Univ. of Illinois, Illinois State Water Survey	Univ. of Veszprem, Veszprem, Hungary	Univ. of Colorado, Boulder	Univ. of Washington
Status	Operational Aug. 1992	Expected to be operational July 1994	Expected to be operational Sept. 1994	Site feasibility measurements began Nov. 1993	Operational May 1993
Sample RH	RH <40%	RH<40%	RH<40%	Uncontrolled	RH<40%
Sample size	$D_p < 1 \mu\text{m}$	$D_p < 1 \mu\text{m}$	$D_p < 1 \mu\text{m}$	Uncontrolled	$D_p < 1 \mu\text{m}$
Fractions	$1 < D_p < 10 \mu\text{m}$	$1 < D_p < 10 \mu\text{m}$			$1 < D_p < 10 \mu\text{m}$
Optical measurements	$\sigma_{sp}(3\lambda)$, $\delta(4\lambda)$	$\sigma_{sp}(1\lambda)$	$\sigma_{ap}(1\lambda)$, $\sigma_{sp}(1\lambda)$, $\delta(4\lambda)$	$\sigma_{sp}(1\lambda)$	$\sigma_{ap}(1\lambda)$, $\sigma_{sp}(1\lambda)$, $\sigma_{bsp}(1\lambda)$
Microphysical measurements	N_{tot}	N_{tot}	N_{tot}	N_{tot}	N_{tot}
Chemical measurements	Major ions	Major ions	Major ions	None	Major ions

A limited sampling program was conducted from April 1993 to March 1994 to evaluate the suitability for long-term, ground based, aerosol measurements of the proposed monitoring site outside of Laramie, Wyoming. This site was chosen because vertical profiles of aerosol size distribution have regularly been obtained by the University of Wyoming for the last 20 years at this site. However, 12 months of surface measurements of σ_{sp} and N_{tot} revealed that the site is very frequently contaminated by local sources in the Laramie Valley, making it unrepresentative as a clean continental monitoring site. Consequently, measurements of σ_{sp} and N_{tot} were initiated in November 1993 to evaluate the feasibility of using the University of Colorado's facility on Niwot Ridge as a clean continental site. Initial results from this site are promising, although transport of polluted air from metropolitan Denver occurs regularly during afternoon, upslope flow conditions in the summer.

The Cheeka Peak site is operated independently by the University of Washington with major funding from the

NOAA Climate and Global Change Program. Although the sampling protocols are essentially identical to those used at the other CMDL sites, all data acquisition and processing is the responsibility of the University of Washington. Eventually, data from this site will be included in the CMDL archive and tabulated in a future CMDL Summary Report.

Summary results for Sable Island for 1992 and 1993 are shown in Figure 3.3 (daily geometric means) and Tables 3.3 and 3.4 (monthly geometric means). Table 3.5 contains statistics on the measured parameters at Sable Island (August 1992-June 1994) for three categories: all cases, and those cases when both N_{tot} and σ_{sp} (550 nm, $D < 1 \mu\text{m}$) are below and above, respectively, one standard deviation of their mean value ("clean" and "dirty," respectively). These criteria correspond to $N_{tot} < 398 \text{ cm}^{-3}$ and $\sigma_{sp} < 5.0 \text{ Mm}^{-1}$ (clean) and $N_{tot} > 2089 \text{ cm}^{-3}$ and $\sigma_{sp} > 22.9 \text{ Mm}^{-1}$ (dirty). The Sable Island site was chosen to provide information on the properties of pollution aerosols subsequent to long-range transport from the continent, as

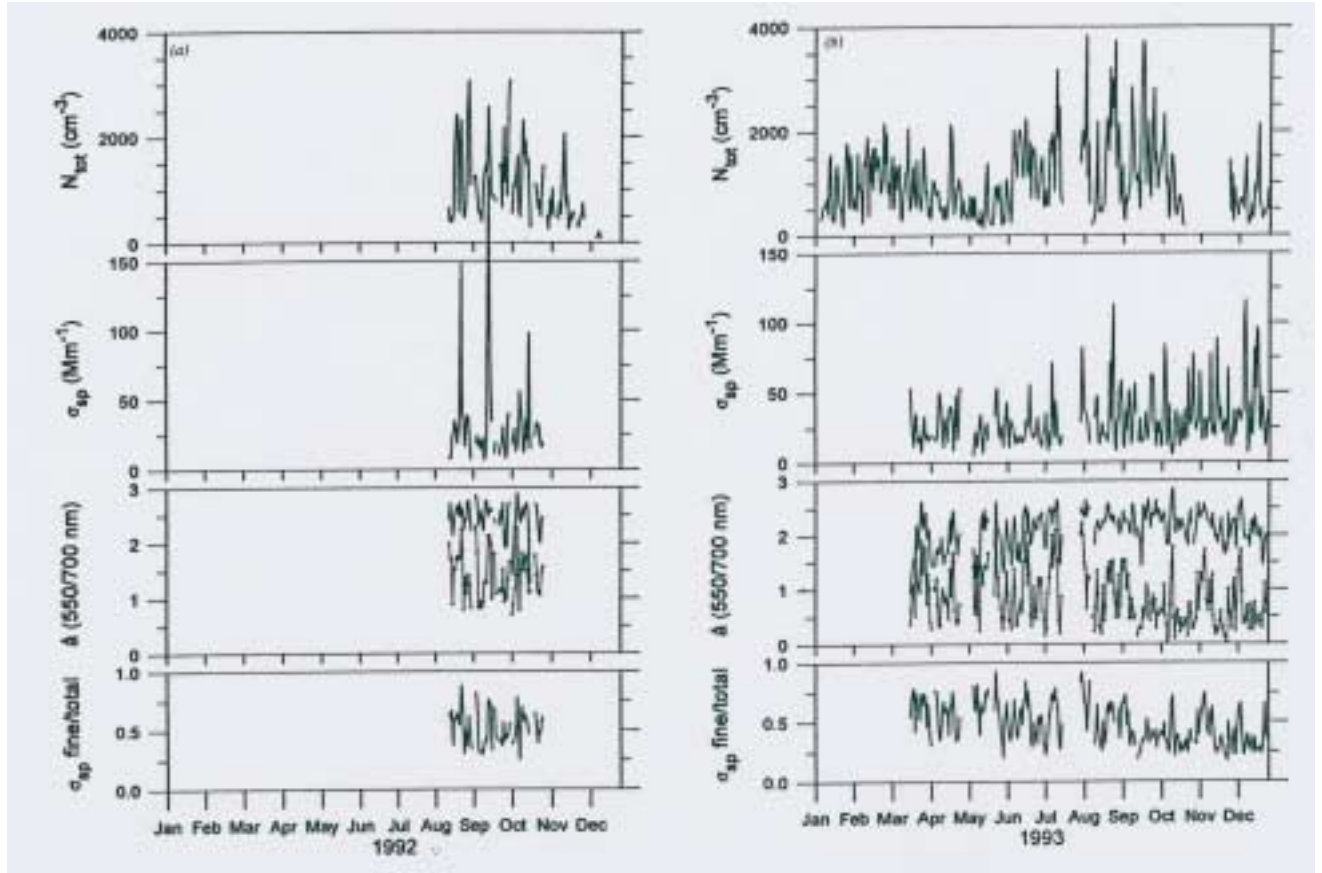


Fig. 3.3. Daily mean aerosol properties at Sable Island (a) 1992 and (b) 1993. Values of σ_{sp} are measured at 550 nm wavelength.

TABLE 3.3. Sable Island Monthly Means for 1992

Parameter	Maximum Diameter (μm)	Wavelength (nm)	Units	Aug.	Sept.	Oct.	Nov.	Dec.
N_{tot}	All		cm^{-3}	944	1135	1100	591	183
σ_{sp}	10	450	Mm^{-1}	29.7	24.3	26.9	N/A	N/A
σ_{sp}	10	550	Mm^{-1}	26.0	21.8	23.8	N/A	N/A
σ_{sp}	10	700	Mm^{-1}	17.8	15.8	17.1	N/A	N/A
σ_{sp}	1	450	Mm^{-1}	18.8	13.5	16.9	N/A	N/A
σ_{sp}	1	550	Mm^{-1}	14.2	10.0	12.6	N/A	N/A
σ_{sp}	1	700	Mm^{-1}	7.7	5.4	7.1	N/A	N/A

TABLE 3.4: Sable Island Monthly Means for 1993

Parameter	Maximum Diameter (μm)	Wavelength (nm)	Units	Jan.	Feb.	March	April	May	June	July	Aug.	Sept.	Oct.	Nov.	Dec.
N_{tot}	All		cm^{-3}	693	1064	871	641	425	1050	1188	1167	1265	842	1441	585
σ_{sp}	10	450	Mm^{-1}	N/A	N/A	25.9	27.5	25.0	24.8	25.0	33.5	32.3	25.6	34.4	35.4
σ_{sp}	10	550	Mm^{-1}	N/A	N/A	21.6	24.4	20.7	21.5	20.9	28.3	28.7	23.2	30.9	32.5
σ_{sp}	10	700	Mm^{-1}	N/A	N/A	16.3	20.0	15.8	17.5	16.1	21.9	23.9	20.3	26.3	27.6
σ_{sp}	1	450	Mm^{-1}	N/A	N/A	18.6	16.9	17.7	14.3	14.1	22.1	17.1	11.8	16.4	15.3
σ_{sp}	1	550	Mm^{-1}	N/A	N/A	13.8	12.8	12.9	10.4	9.8	15.4	12.0	8.1	11.5	11.0
σ_{sp}	1	700	Mm^{-1}	N/A	N/A	8.7	8.2	8.0	6.4	5.7	8.7	6.9	4.7	6.8	6.6

TABLE 3.5. Mean Observed Values at Sable Island (August 1992-June 1994)

Parameter	Maximum Diameter (μm)	Wavelength (nm)	Units	Clean Cases	All Cases	Dirty Cases
N_{tot}	All		cm^{-3}	245	912	2884
σ_{sp}	10	450	Mm^{-1}	9.8	28.8	93.3
σ_{sp}	1	450	Mm^{-1}	4.3	15.1	63.1
σ_{sp}	10	550	Mm^{-1}	8.7	25.1	74.1
σ_{sp}	1	550	Mm^{-1}	3.0	10.7	43.7
σ_{sp}	10	700	Mm^{-1}	7.2	20.0	51.3
σ_{sp}	1	700	Mm^{-1}	1.8	6.3	24.0
\AA	10	450/550	None	0.49	0.69	1.17
\AA	1	450/550	None	1.76	1.79	1.93
\AA	10	550/700	None	0.74	0.91	1.49
\AA	1	550/700	None	2.12	2.19	2.47
$\sigma_{\text{sp fine/total}}$	1+10	450	None	0.48	0.56	0.70
$\sigma_{\text{sp fine/total}}$	1+10	550	None	0.38	0.46	0.62
$\sigma_{\text{sp fine/total}}$	1+10	700	None	0.30	0.36	0.51

Notes: (1) The Ångström exponent is denoted \AA to avoid confusion in the future with the mass scattering efficiency α . (2) The entries for " $\sigma_{\text{sp fine/total}}$ " are the fraction of the total aerosol light scattering coefficient attributable to submicrometer particles. (3) Geometric means are reported for N_{tot} and σ_{sp} , while arithmetic means are reported for \AA and $\sigma_{\text{sp fine/total}}$. (4) Clean and dirty cases are those hours when both N_{tot} and σ_{sp} (550 nm, $D < 1 \mu\text{m}$) are below and above, respectively, one standard deviation of the mean value.

well as information on aerosols in the clean marine boundary layer. The initial results reflect the different transport patterns influencing the site, with periods of low aerosol number concentration and light scattering coefficient interspersed with periods of high aerosol loadings. Trajectory analyses of a limited number of cases reveal that transport from the south and southeast (clean marine) is associated with low aerosol loadings, and that trajectories from the west and southwest (polluted continental) are associated with high aerosol loadings. Monthly mean aerosol loadings are considerably higher than the levels encountered at the CMDL baseline stations because of the proximity of Sable Island to continental pollution sources.

Inclusion of size- and wavelength-dependence of σ_{sp} in the sampling protocol allows identification of systematic shifts in the aerosol size distribution under different conditions (Table 3.5). Fine particles (diameter $< 1 \mu\text{m}$) are responsible for less than half of the aerosol light scattering (550-nm wavelength), and this fraction systematically increases from clean to dirty conditions. Similarly, the Ångström exponent \AA

systematically increases from clean to dirty conditions, for both fine and total size fractions. Together, these two findings indicate that fine particles are systematically smaller, and more abundant, under dirty conditions. Linear regression analysis demonstrates that 75% of the variance in the Ångström exponent (total size fraction) can be explained by variance in the fraction of light scattering caused by fine particles (550 nm wavelength), i.e., the major factor controlling \AA is the relative abundance of fine and coarse particles (diameter $> 1 \mu\text{m}$).

Information and data from the aerosol group at CMDL is now available on the Internet by FTP and World Wide Web (WWW) servers. Recently processed data, file format specifications, documents summarizing data processing and flow, and clean processed data presented in hourly averaged files for all years of station operation are available by anonymous FTP to <ftp.cmdl.noaa.gov>, directory "aerosol." In addition to the above, the CMDL WWW server at <http://www.cmdl.noaa.gov> supplies online plots of recently processed aerosol data and hypertext links to various related documents.